

**Bisisoindigo: using a ring-fusion approach to extend the conjugation length of  
isoindigo**

Nicholas M. Randell, Philip C. Boutin, Timothy L. Kelly\*

Department of Chemistry, University of Saskatchewan,

110 Science Place, Saskatoon, Saskatchewan, Canada, S7N 5C9

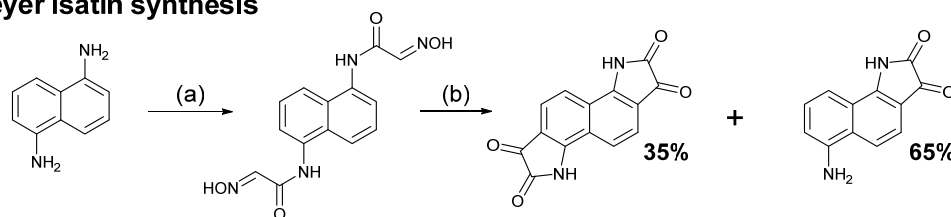
E-mail: [tim.kelly@usask.ca](mailto:tim.kelly@usask.ca), Fax: (306) 966-4730, Phone: (306) 966-4666

**Contents:**

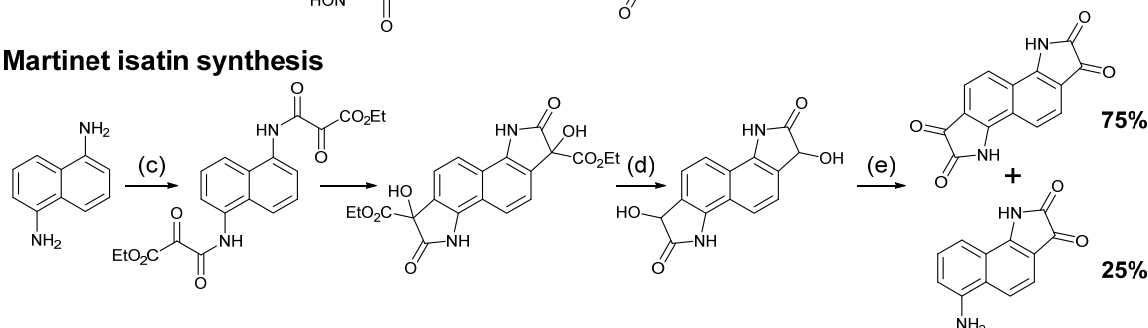
- 1. Martinet and Sandmeyer bisisatin syntheses**
- 2. Detailed experimental procedures**
- 3. OPV optimization**
- 4. Atomic force microscopy imaging of active layer blends**
- 5. Solid state UV/vis spectroscopy of OPV active layer blends**
- 6. Fluorescence quenching in donor/acceptor solutions**
- 7.  $^1\text{H}$  NMR and  $^{13}\text{C}$  NMR spectra**
- 8. References**

## 1. Martinet and Sandmeyer bisisatin syntheses

### Sandmeyer isatin synthesis



### Martinet isatin synthesis



**Scheme S1.** Sandmeyer and Martinet isatin syntheses. (a) C(OH)<sub>2</sub>CCl<sub>3</sub>, NH<sub>3</sub>OHCl, (b) H<sub>2</sub>SO<sub>4</sub>, (c) diethylketomalonate, glacial acetic acid, (d) NaOH, H<sub>2</sub>O, (e) sparging air.

## 2. Detailed experimental procedures

### Synthesis

2-Ethylhexyl iodide and 5-hexyl-5'-tertbutylstannyl-2,2'-bithiophene were synthesized according to previously reported methods.<sup>1,2</sup>

### Synthesis of 1-(2-ethylhexyl)-isatin (**S1**)

The synthetic procedure was adapted from a previous literature report.<sup>3</sup> Isatin (2.00 g, 13.6 mmol) and K<sub>2</sub>CO<sub>3</sub> (2.25 g, 16.3 mmol) were dissolved in 50 mL of DMF and the mixture was heated to 100 °C. 2-Ethylhexyl bromide (3.0 mL, 16.8 mmol) was added via syringe and the resulting mixture was stirred at 100 °C for 18 hours. The reaction mixture was poured over ice and extracted with CH<sub>2</sub>Cl<sub>2</sub>. The combined organic layers were washed with brine, dried over MgSO<sub>4</sub> and concentrated. The resulting orange solid was heated to 90 °C *in vacuo* to remove excess 2-ethylhexyl bromide, yielding **S1** as an orange oil (3.11 g, 88%). <sup>1</sup>H NMR (500 MHz, CDCl<sub>3</sub>, δ): 7.55-7.62 (m, 2H), 7.11 (t, *J* = 7.5 Hz, 1H), 6.87 (d, *J* = 7.9 Hz, 1H), 3.56-3.65 (m, 2H), 1.78-1.85 (m, 1H), 1.24-1.42 (m, 8H), 0.94 (t, *J* = 7.5 Hz), 0.89 (t, *J* = 7.1 Hz). <sup>13</sup>C NMR (125 MHz, CDCl<sub>3</sub>, δ): 183.82, 158.68, 151.69, 138.45, 125.59, 123.75, 117.83, 110.57, 44.57, 37.54, 30.81, 28.81, 24.16,

23.21, 14.23, 10.76. HRMS ( $m/z$ ) ( $M^+$ ): Calc ( $C_{16}H_{21}NO_2$ ): 259.15723 Found: 259.15691. Anal. Calcd for  $C_{16}H_{21}NO_2$ : C, 74.10; H, 8.16; N, 5.40; Found: C, 73.86; H, 7.91; N, 5.38.

#### Synthesis of 6-bromo-1-(2-ethylhexyl)-isatin (**S2**)

6-Bromoisatin was reacted with 2-ethylhexyl bromide following the same procedure as for the synthesis of **S1**, yielding **S2** as an orange solid (1.38 g, 46%). m.p. 62-64 °C.  $^1H$  NMR (500 MHz,  $CDCl_3$ ,  $\delta$ ): 7.46 (d,  $J$  = 8.0 Hz, 1H), 7.27 (d, 8.0 Hz, 1H), 7.03 (s, 1H), 3.54-3.63 (m, 2H), 1.77-1.82 (m, 1H), 1.29-1.41 (m, 9H), 0.94 (t,  $J$  = 7.5 Hz, 3H), 0.90 (t,  $J$  = 7.0 Hz, 3H).  $^{13}C$  NMR (125 MHz,  $CDCl_3$ ,  $\delta$ ): 182.4, 158.4, 152.4, 133.6, 126.9, 126.5, 116.4, 114.1, 44.7, 37.3, 30.6, 28.5, 24.0, 23.1, 14.1, 10.6. HRMS ( $m/z$ ) ( $M^+$ ): Calc ( $C_{16}H_{20}NO_2Br$ ): 337.06774 Found: 337.06652. Anal. Calcd for  $C_{16}H_{20}NO_2Br$ : C, 56.82; H, 5.96; N, 4.14; Found: C, 57.39; H, 5.97; N, 4.23.

#### Synthesis of 1-(2-ethylhexyl)-2-oxindole (**4**)

The synthetic procedure was based on an adaptation of previously reported procedures.<sup>4, 5</sup> **S1** (3.11 g, 12.0 mmol) was suspended in 20 mL of hydrazine hydrate and the reaction mixture was heated at reflux for 4 hours. The reaction mixture was cooled and extracted with EtOAc. The combined organic layers were dried over  $MgSO_4$  and concentrated to yield a yellow solid. Metallic sodium (0.86 g) was dissolved in 40 mL of anhydrous EtOH. The yellow solid was transferred into the EtOH/NaOEt solution using anhydrous EtOH and the reaction mixture was heated at reflux for 2 hours. The resulting brown solution was poured over ice and acidified with aqueous 1 mol  $L^{-1}$  HCl. The suspension was extracted with EtOAc and the combined organic layers were washed with brine, dried over  $MgSO_4$ , and concentrated to yield pure 1-(2-ethylhexyl)-2-oxindole as a yellow-orange oil (2.51 g, 85%).  $^1H$  NMR (500 MHz,  $CDCl_3$ ,  $\delta$ ): 7.22-7.28 (m, 3H), 7.02 (t,  $J$  = 7.5 Hz, 1H), 6.81 (t,  $J$  = 7.5 Hz, 1H), 3.54-2.64 (m, 2H), 3.53 (s, 1H), 1.79-1.84 (m, 1H), 1.23-1.40 (m, 13H), 0.92 (t,  $J$  = 7.5 Hz, 3H), 0.88 (t,  $J$  = 7.0 Hz, 3H).  $^{13}C$  NMR (125 MHz,  $CDCl_3$ ,  $\delta$ ): 175.4, 145.1, 127.8, 124.7, 124.4, 122.0, 108.6, 44.1, 37.4, 35.8, 30.7, 28.7, 24.0, 23.1, 14.1, 10.7. HRMS ( $m/z$ ) ( $M^+$ ): Calc ( $C_{16}H_{23}NO$ ): 245.17796 Found: 245.17699. Anal. Calcd for  $C_{16}H_{23}NO$ : C, 78.32; H, 9.45; N, 5.71; Found: C, 77.98; H, 9.61; N, 5.95.

### Synthesis of 6-bromo-1-(2-ethylhexyl)-2-oxindole (5)

**S2** was reacted with hydrazine hydrate and NaOEt/EtOH following the same procedure as **4** to yield an orange-red solid (1.33 g, quantitative yield). m.p. 46-48 °C. <sup>1</sup>H NMR (500 MHz, CDCl<sub>3</sub>, δ): 7.15 (d, *J* = 7.80 Hz, 1H), 7.09 (d, *J* = 7.85 Hz, 1H), 6.93 (s, 1H), 3.51-3.58 (m, 2H), 3.46 (s, 2H), 1.77-1.82 (m, 1H), 1.24-1.34 (m, 12H), 0.88-0.94 (m, 7H). <sup>13</sup>C NMR (125 MHz, CDCl<sub>3</sub>, δ): 175.2, 146.5, 125.7, 125.0, 123.5, 121.4, 112.1, 44.4, 37.3, 35.5, 30.6, 28.7, 24.0, 23.2, 14.2, 10.7. HRMS (*m/z*) (*M*<sup>+</sup>) Calc (C<sub>16</sub>H<sub>22</sub>NOBr): 323.08848, Found: 323.08762. Anal. Calcd for C<sub>16</sub>H<sub>22</sub>NOBr: C, 59.27; H, 6.84; N, 4.32; Found: C, 59.45; H, 6.81; N, 5.19.

### OPV fabrication and testing

ITO-coated glass substrates (Delta Technologies, *R<sub>s</sub>* = 15-25 Ω/□) were cleaned by sequential sonication in: 10% (v/v) Extran detergent in Millipore H<sub>2</sub>O, Millipore H<sub>2</sub>O, acetone and isopropanol. Cleaned substrates were stored under isopropanol until use. Substrates were blown dry with compressed air and UV/ozone cleaned for 15 min immediately prior to use. Poly(3,4-ethylenedioxythiophene:polystyrene sulfonate (Clevios P VP AI 4083) solutions were mixed with 0.5% v/v Zonyl F-300 fluoro-surfactant (40% solids in H<sub>2</sub>O) and filtered through a 0.45 μm syringe filter. The solution was then spin cast onto the ITO substrates and annealed at 125 °C for 10 min before being placed in a N<sub>2</sub> atmosphere glovebox. Active layer solutions were prepared at a 1:1 donor:acceptor ratio (by mass), and were stirred overnight and syringe filtered using a 0.45 μm filter before use. 1,8-Diiodooctane (DIO) was added after filtration. Active layers were spin cast at either 5000 rpm (CHCl<sub>3</sub>) or 1000 rpm (*o*-dichlorobenzene and chlorobenzene). Residual solvent was allowed to evaporate at room temperature for 1 hour before electrode deposition. LiF (0.8 nm) and Al (100 nm) were then thermally evaporated onto the substrates at a base pressure of 3 × 10<sup>-6</sup> mbar.

Current-voltage measurements were made inside a N<sub>2</sub> atmosphere glovebox using a Keithley 2400 source-measure unit. The cells were illuminated by a 450 W Class AAA solar simulator equipped with an AM1.5G filter (Sol3A, Oriel instruments) at a calibrated intensity of 100 mW cm<sup>-2</sup>, as determined by a standard silicon reference cell (91150V,

Oriel Instruments). The cell area was defined by a non-reflective anodized aluminium mask to be 0.0708 cm<sup>2</sup>. Incident photon-to-current efficiency (IPCE) measurements were performed on the highest efficiency devices in a N<sub>2</sub> atmosphere using a QE-PV-SI system (Oriel Instruments) consisting of a 300 W Xe arc lamp, monochromator, chopper, lock-in amplifier and certified silicon reference cell. Measurements were made using a 30 Hz chop frequency.

### **Fluorescence quenching and quantum yield measurements**

Fluorescence spectra for quenching and quantum yield experiments were measured using a Photon Technology International QuantaMaster spectrofluorometer. Data were smoothed by a Savitzky-Golay algorithm. Fluorescence-quenching experiments were performed by titrating solutions of P3HT or PTB7-Th with either **6** or **8**. In all cases the donor concentration was held fixed at 45 µg/mL while the acceptor concentration was increased from 0 to ~45 µg/mL.

### **(TD)DFT procedures and results**

DFT and TDDFT calculations were carried out, using the Gaussian 09 and Gaussview suites of software,<sup>6</sup> at a B3LYP/6-31G(d,p) level of theory using a chloroform dielectric continuum model. Alkyl substituents on **6** and **8** were replaced with methyl groups in order to simplify the calculations. The UV/vis spectra were calculated using the SWizard program, revision 5.0, using the (Gaussian/Lorentzian/pseudo-Voigt) model.<sup>7,8</sup>

### 3. OPV optimization

**Table S1:** Device performance parameters for OPV devices fabricated with PTB7-Th:6 active layers spin cast from 1,2-dichlorobenzene.

Conditions	$V_{oc}$ (V)	$J_{sc}$ (mA/cm <sup>2</sup> )	Fill Factor	Efficiency (%)
<b>20 mg/mL</b>				
average	$0.4 \pm 0.3$	$0.051 \pm 0.004$	$28 \pm 2$	$0.006 \pm 0.004$
best	0.73	0.056	28	0.0112
<b>20 mg/mL + 1% v/v DIO</b>				
average	$0.6 \pm 0.3$	$0.24 \pm 0.04$	$28 \pm 1$	$0.04 \pm 0.02$
best	0.98	0.27	29	0.075
<b>20 mg/mL + 2% v/v DIO</b>				
average	$0.7 \pm 0.3$	$0.27 \pm 0.04$	$30 \pm 2$	$0.05 \pm 0.03$
best	1.0	0.33	31	0.10
<b>20 mg/mL + 3% v/v DIO</b>				
average	$0.7 \pm 0.4$	$0.27 \pm 0.04$	$29 \pm 2$	$0.05 \pm 0.03$
best	1.00	0.29	29	0.086

**Table S2:** Device performance parameters for OPV devices fabricated with PTB7-Th:8 active layers spin cast from chloroform.

Conditions	$V_{oc}$ (V)	$J_{sc}$ (mA/cm <sup>2</sup> )	Fill Factor	Efficiency (%)
<b>20 mg/mL 1% v/v DIO</b>				
average	$0.5 \pm 0.2$	$0.027 \pm 0.002$	$27 \pm 1$	$0.003 \pm 0.001$
best	0.60	0.030	27	0.0048
<b>20 mg/mL 1% v/v DIO annealed</b>				
average	$0.4 \pm 0.1$	$0.031 \pm 0.003$	$26 \pm 1$	$0.003 \pm 0.001$
best	0.53	0.032	24	0.0041
<b>20 mg/mL</b>				
average	$0.4 \pm 0.2$	$0.016 \pm 0.002$	$28 \pm 3$	$0.0017 \pm 0.0006$
best	0.51	0.02	27	0.0025
<b>20 mg/mL annealed</b>				
average	$0.4 \pm 0.1$	$0.69 \pm 0.09$	$36 \pm 4$	$0.10 \pm 0.03$
best	0.48	0.021	26	0.0027

**Table S3:** Device performance parameters for OPV devices fabricated with **6:PC<sub>71</sub>BM** active layers spin cast from chlorobenzene.

Conditions	$V_{oc}$ (V)	$J_{sc}$ (mA/cm <sup>2</sup> )	Fill Factor	Efficiency (%)
<b>20 mg/mL 1% v/v DIO</b>				
average	$0.5 \pm 0.2$	$0.9 \pm 0.1$	$34 \pm 7$	$0.17 \pm 0.07$
best	0.65	1.06	45	0.31
<b>20 mg/mL 1% v/v DIO annealed</b>				
average	$0.25 \pm 0.09$	$0.24 \pm 0.04$	$30 \pm 3$	$0.018 \pm 0.008$
best	0.38	0.29	31	0.035
<b>40 mg/mL 1% v/v DIO</b>				
average	$0.5 \pm 0.2$	$0.09 \pm 0.06$	$22 \pm 9$	$0.009 \pm 0.006$
best	0.27	0.17	37	0.017
<b>20 mg/mL 3% v/v DIO</b>				
average	$0.4 \pm 0.1$	$0.69 \pm 0.09$	$36 \pm 4$	$0.10 \pm 0.03$
best	0.51	0.81	40	0.17
<b>20 mg/mL</b>				
average	$0.69 \pm 0.04$	$0.04 \pm 0.05$	$25 \pm 7$	$0.01 \pm 0.01$
best	0.73	0.10	36	0.026

**Table S4:** Device performance parameters for OPV devices fabricated with **8:PC<sub>71</sub>BM** active layers spin cast from chloroform.

Conditions	$V_{oc}$ (V)	$J_{sc}$ (mA/cm <sup>2</sup> )	Fill Factor	Efficiency (%)
<b>20 mg/mL</b>				
average	$0.4 \pm 0.2$	$0.09 \pm 0.03$	$30 \pm 6$	$0.010 \pm 0.007$
best	0.57	0.12	33	0.02
<b>20 mg/mL 1% v/v DIO</b>				
average	$0.54 \pm 0.09$	$0.61 \pm 0.09$	$22 \pm 4$	$0.08 \pm 0.06$
best	0.59	1.28	30	0.23
<b>20 mg/mL 3% v/v DIO</b>				
average	$0.43 \pm 0.06$	$0.026 \pm 0.008$	$15 \pm 2$	$0.0017 \pm 0.0006$
best	0.51	0.046	14	0.0033

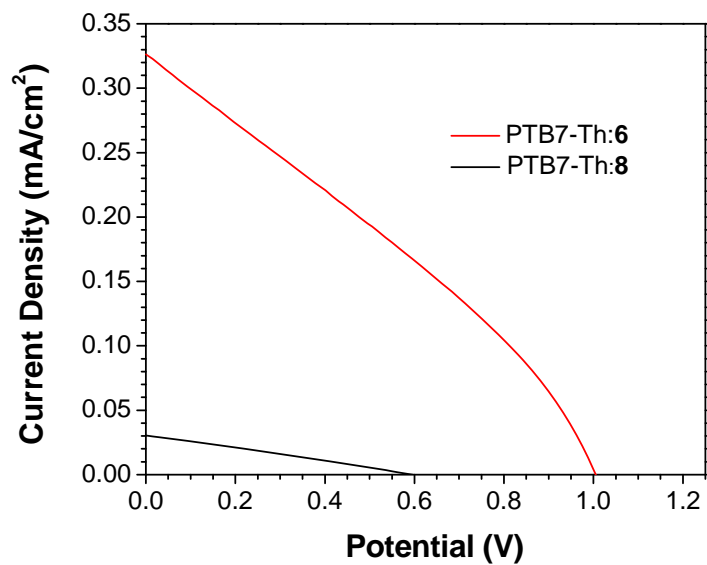


**Figure S1.** Current-voltage curves of the best devices fabricated with PTB7-Th:6 and PTB7-Th:8 active layers.

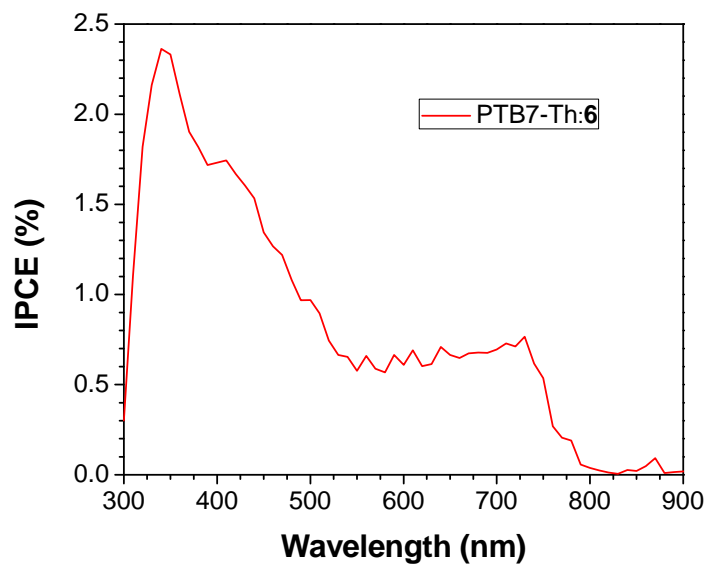


**Figure S2.** IPCE spectrum of a representative OPV device fabricated with a PTB7-Th:6 active layer.



#### 4. Atomic force microscopy imaging of active layer blends

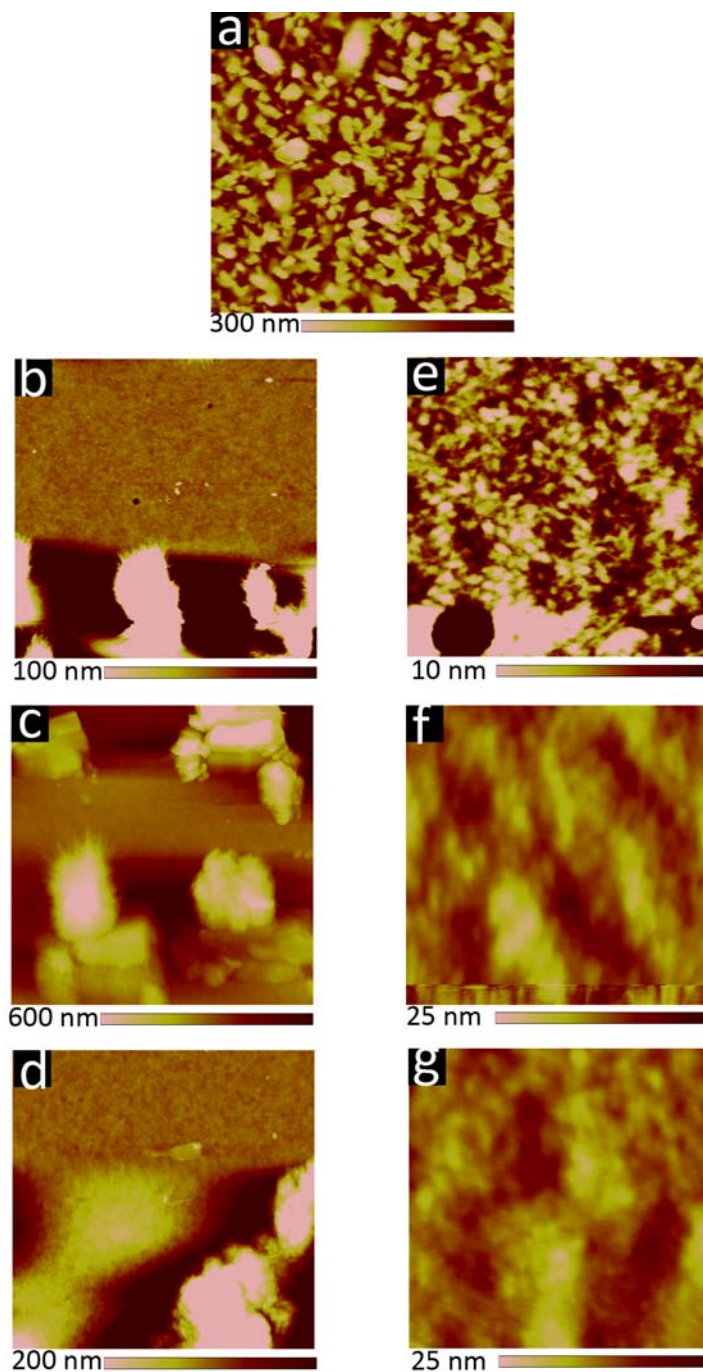


**Figure S3.** AFM images of PTB7-Th:6 active layer blends cast from 20 mg/mL solutions containing: (a) 0%, (b,e) 1% , (c,f) 2%, (d,g) 3% DIO. Images (a-d) are 10 μm × 10 μm, images (e-g) are 1 μm × 1 μm.

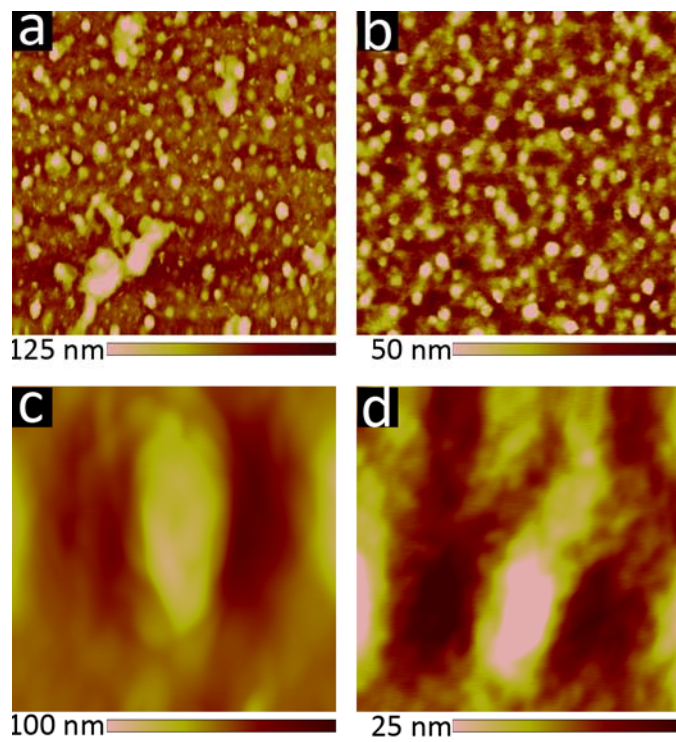


**Figure S4.** AFM images of PTB7-Th:**8** active layer blends cast from 20 mg/mL solutions containing:(a,c) 0%, (b,d) 1% DIO. Images (a-b) are 10  $\mu\text{m}$   $\times$  10  $\mu\text{m}$ , images (c-d) are 1  $\mu\text{m}$   $\times$  1  $\mu\text{m}$ .

## 5. Solid state UV/vis spectroscopy of OPV active layer blends

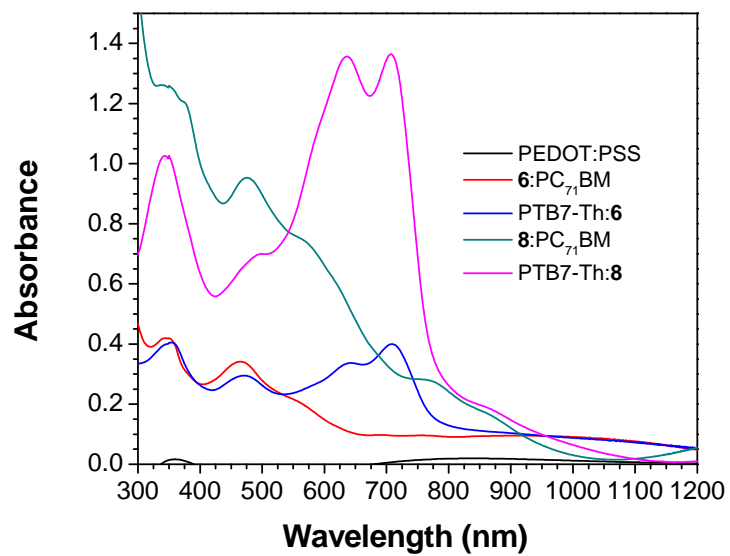


**Figure S5.** UV/vis spectra of active layers on Glass/ITO/PEDOT:PSS substrates.

## 6. Fluorescence quenching in donor/acceptor solutions

### Calculation of fluorescence quantum yields

Fluorescence quantum yields of P3HT and PTB7-Th in chloroform were calculated via the comparative method,<sup>9</sup> taking

$$\Phi_F^x = \Phi_F^s \frac{1 - 10^{A_{\lambda_{\text{ex}}}^s} \int F^x(\lambda_{\text{em}}) n_x^2}{1 - 10^{A_{\lambda_{\text{ex}}}^x} \int F^s(\lambda_{\text{em}}) n_s^2}$$

where x is the compound under study, s is the reference standard, and  $\Phi_F$ , A,  $F(\lambda_{\text{em}})$ , and n are the fluorescence quantum yield, absorption, fluorescence spectrum, and solvent refractive index, respectively. The sample and reference standard were excited at the same wavelength, far removed from any fluorescence features. Fluorescence spectra were corrected for reabsorption. Rhodamine 6G in chloroform, which has a fluorescence quantum yield of 0.75,<sup>10</sup> was used as the reference standard for P3HT. The fluorescence quantum yield of P3HT in chloroform was measured as 0.22, which is comparable to the previously reported value of  $0.33 \pm 0.07$  in chlorobenzene.<sup>11</sup> Chlorophyll a in methanol ( $\Phi_F = 0.15$ )<sup>12</sup> was used as the reference standard for PTB7-Th. The fluorescence quantum yield of PTB7-Th in chloroform was measured as 0.042, which is comparable to the previously recorded value of 0.02 for PTB7 in chlorobenzene.<sup>13</sup> To our knowledge, the fluorescence quantum yield of PTB7-Th has not been previously reported. Uncertainty in calculated quantum yield values is estimated as  $\pm 10\%$ .

### Stern-Volmer analysis of fluorescence quenching

Stern-Volmer constants ( $K_{\text{sv}}$ ) for donor-acceptor pairs were determined from the slope of the Stern-Volmer plots (Fig. S6 and S7).

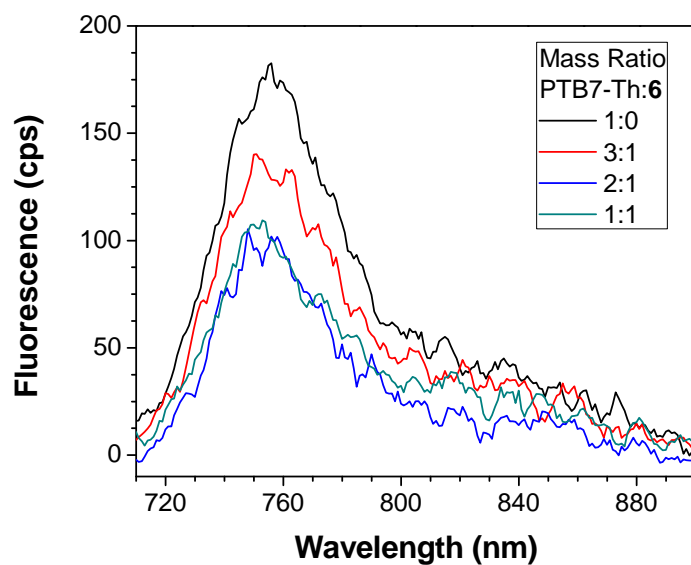


**Figure S6.** Emission spectra of PTB7-Th at various concentrations of **6**.

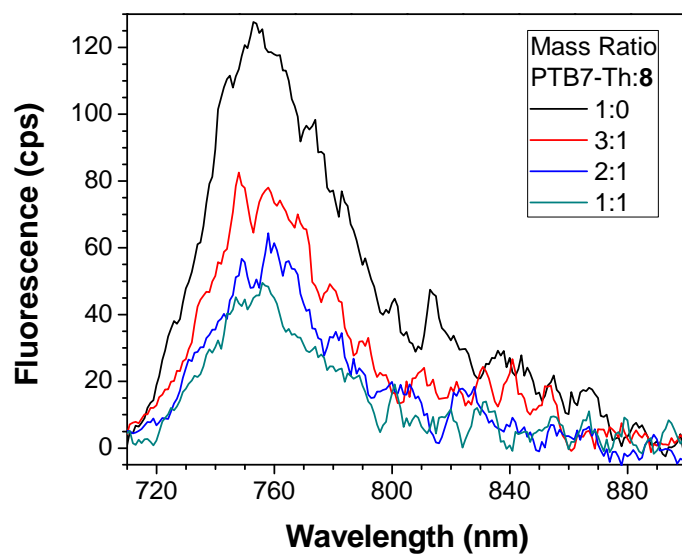


**Figure S7.** Emission spectra of PTB7-Th at various concentrations of **8**.

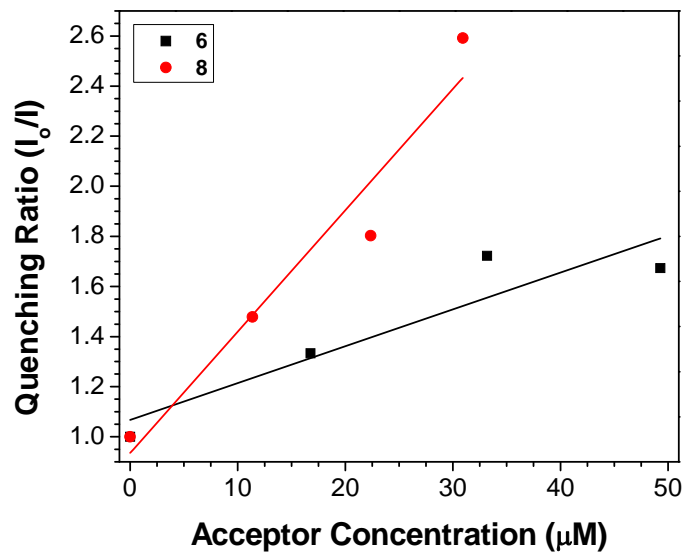


**Figure S8.** Stern-Volmer plot of PTB7-Th fluorescence quenching as a function of acceptor concentration.

**Table S5.** Summary of photophysical data for donor-acceptor blends.

Donor	Acceptor	$\Phi_F^D$	$K_{SV}(\times 10^4 \text{mol}^{-1} \text{L})$
PTB7-Th	<b>6</b>	0.04	$1.5 \pm 0.4$
PTB7-Th	<b>8</b>	0.04	$4.8 \pm 0.8$
P3HT <sup>13</sup>	PC <sub>61</sub> BM <sup>14</sup>		1.6

## 7. $^1\text{H}$ NMR and $^{13}\text{C}$ NMR spectra

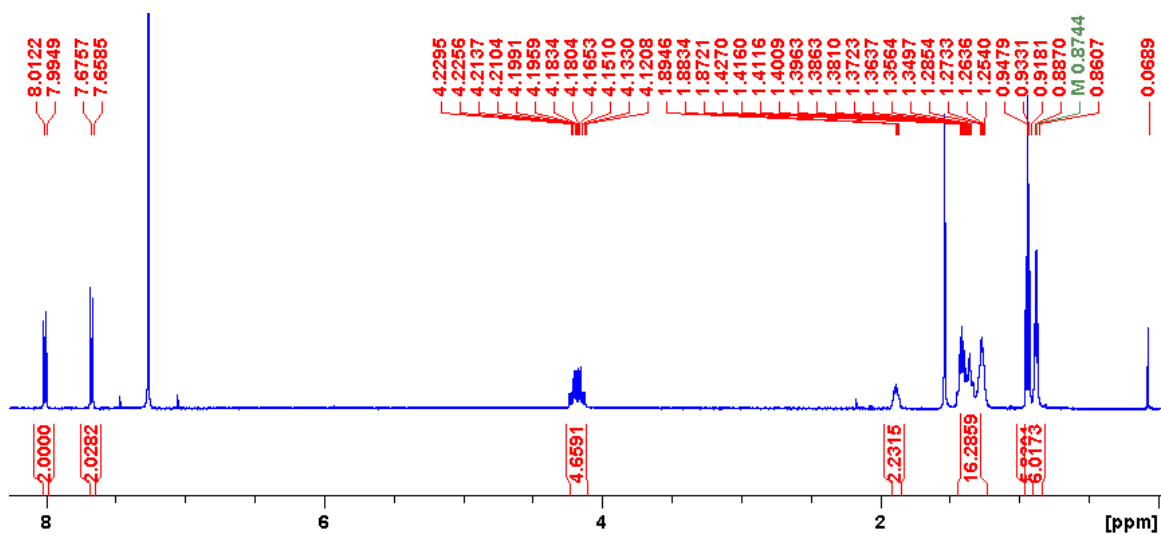


Figure S9.  $^1\text{H}$  NMR spectrum of **3** in  $\text{CDCl}_3$ .

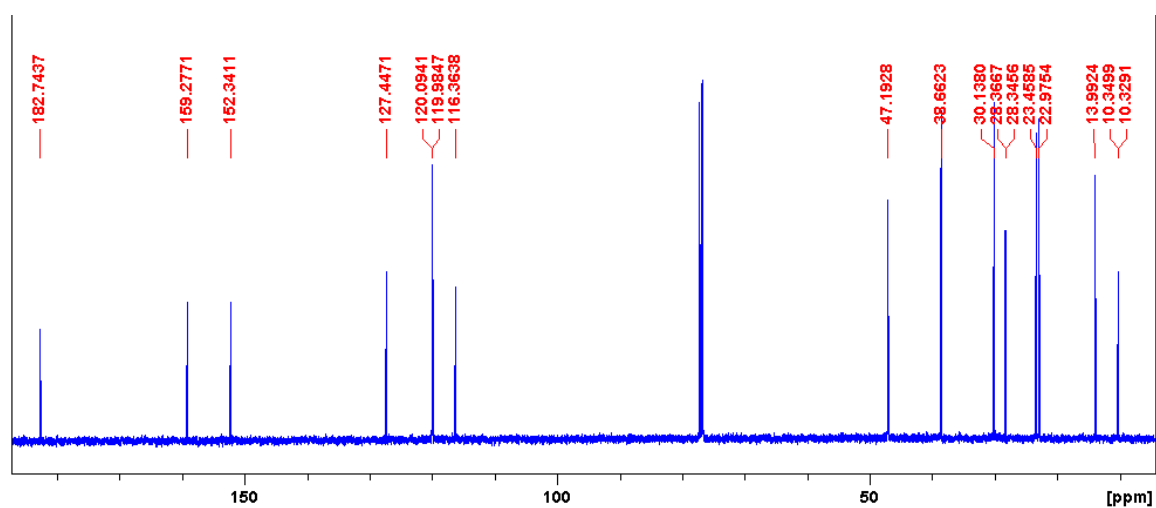
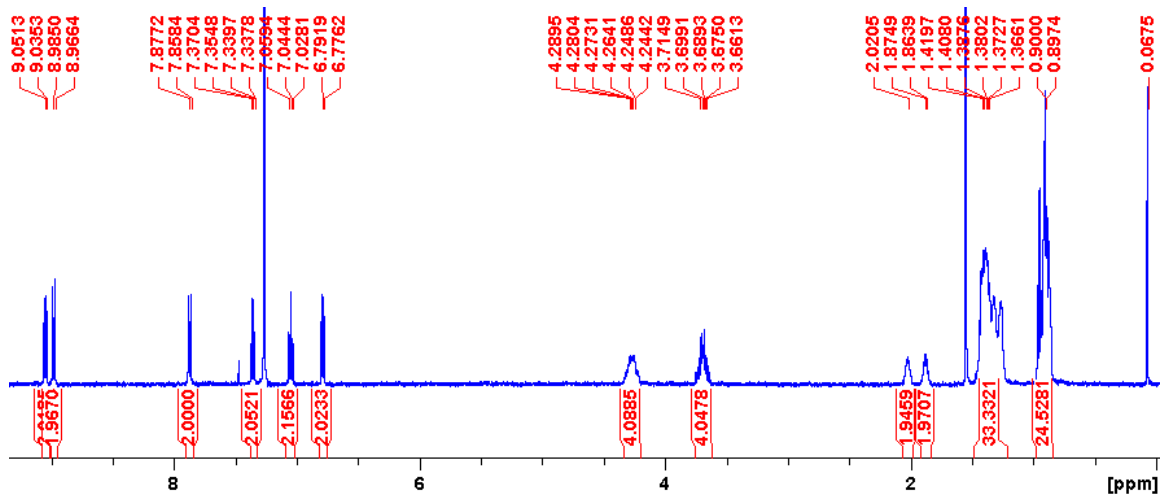
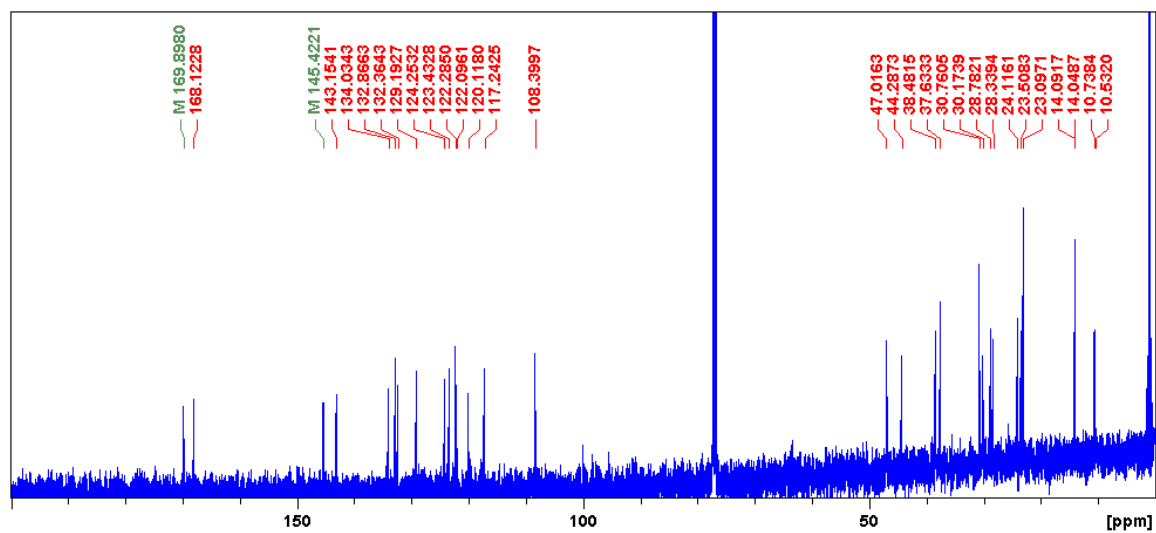


Figure S10.  $^{13}\text{C}$  NMR spectrum of **3** in  $\text{CDCl}_3$ .



**Figure S11.** <sup>1</sup>H NMR spectrum of **6** in CD<sub>2</sub>Cl<sub>2</sub>.



**Figure S12.** <sup>13</sup>C NMR spectrum of **6** in CDCl<sub>3</sub>.



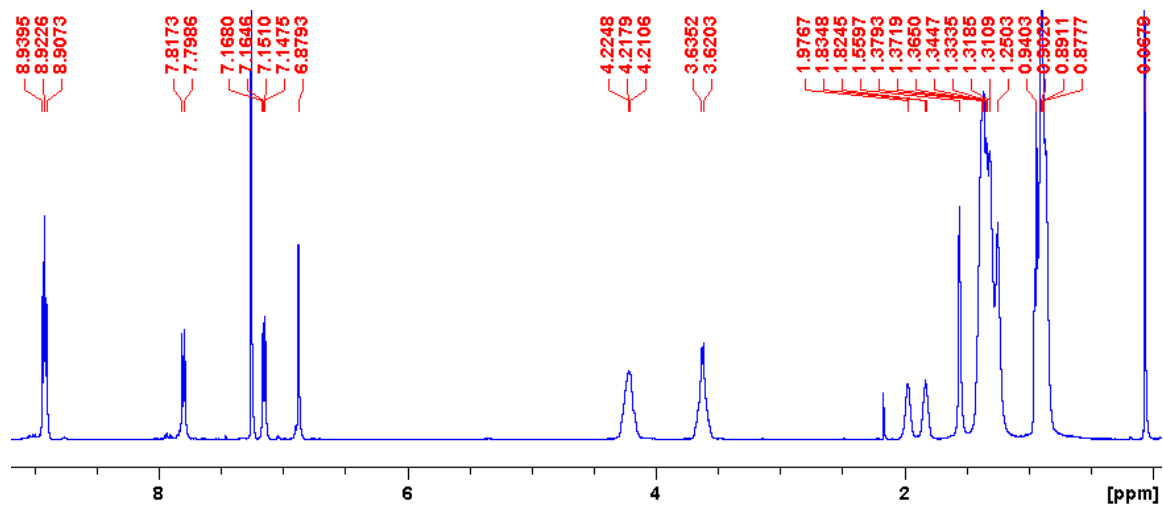


**Figure S13.** <sup>1</sup>H NMR spectrum of **7** in CDCl<sub>3</sub>.

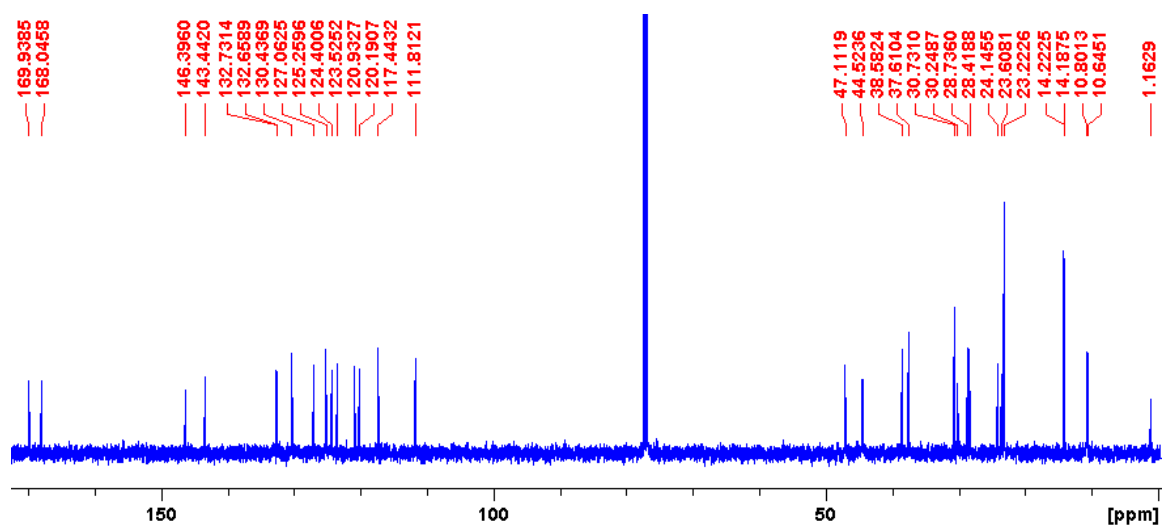


**Figure S14.** <sup>13</sup>C NMR spectrum of **7** in CDCl<sub>3</sub>.

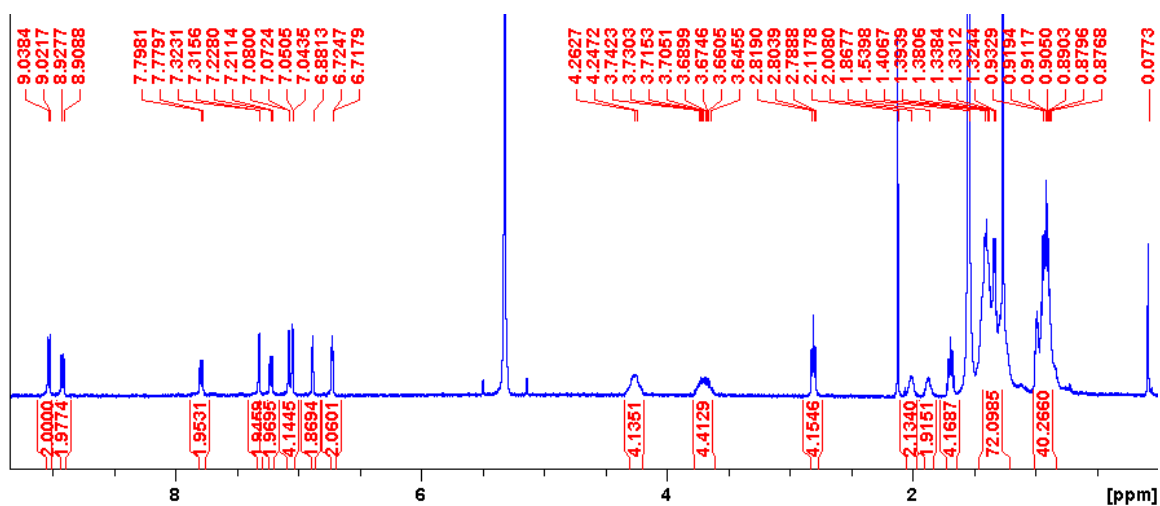


Figure S15. <sup>1</sup>H NMR spectrum of **8** in CD<sub>2</sub>Cl<sub>2</sub>.

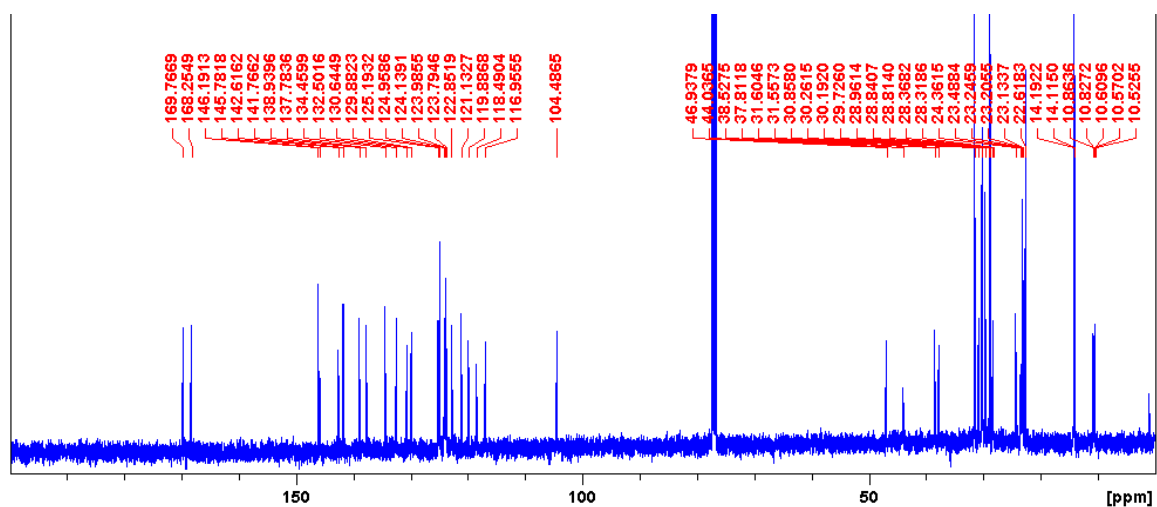


Figure S16. <sup>13</sup>C NMR spectrum of **8** in CDCl<sub>3</sub>.

## 8. References

1. L. Jones, J. S. Schumm, and J. M. Tour, *J. Org. Chem.*, 1997, **62**, 1388–1410.
2. G. Sotgiu, M. Zambianchi, G. Barbarella, and C. Botta, *Tetrahedron*, 2002, **58**, 2245–2251.
3. M. S. Shmidt, A. M. Reverdito, L. Kremenichuzky, I. A. Perillo, M. M. Blanco, *Molecules*, 2008, **13**, 831–840.
4. D. S. Soriano, *J. Chem. Ed.*, 1993, **70**, 332.
5. T. Lei, J.-H. Dou, Z.-J. Ma, C.-H. Yao, C.-J. Liu, J.-Y. Wang, J. Pei, *J. Am. Chem. Soc.*, 2012, **134**, 20025–20028.
6. Gaussian 09, Revision D.01, M. J. Frisch, G. W. Trucks, H. B. Schlegel, G. E. Scuseria, M. A. Robb, J. R. Cheeseman, G. Scalmani, V. Barone, B. Mennucci, G. A. Petersson, H. Nakatsuji, M. Caricato, X. Li, H. P. Hratchian, A. F. Izmaylov, J. Bloino, G. Zheng, J. L. Sonnenberg, M. Hada, M. Ehara, K. Toyota, R. Fukuda, J. Hasegawa, M. Ishida, T. Nakajima, Y. Honda, O. Kitao, H. Nakai, T. Vreven, J. A. Montgomery, Jr., J. E. Peralta, F. Ogliaro, M. Bearpark, J. J. Heyd, E. Brothers, K. N. Kudin, V. N. Staroverov, T. Keith, R. Kobayashi, J. Normand, K. Raghavachari, A. Rendell, J. C. Burant, S. S. Iyengar, J. Tomasi, M. Cossi, N. Rega, J. M. Millam, M. Klene, J. E. Knox, J. B. Cross, V. Bakken, C. Adamo, J. Jaramillo, R. Gomperts, R. E. Stratmann, O. Yazyev, A. J. Austin, R. Cammi, C. Pomelli, J. W. Ochterski, R. L. Martin, K. Morokuma, V. G. Zakrzewski, G. A. Voth, P. Salvador, J. J. Dannenberg, S. Dapprich, A. D. Daniels, O. Farkas, J. B. Foresman, J. V. Ortiz, J. Cioslowski, and D. J. Fox, Gaussian, Inc., Wallingford CT, 2013.
7. S. I. Gorelsky, *SWizard program*, <http://www.sg-chem.net/>, University of Ottawa, Ottawa, Canada, 2013.
8. S. I. Gorelsky, A. B. P. Lever, *J. Organomet. Chem.*, 2001, **635**, 187-196.
9. K. Rurack and M. Spieles, *Anal. Chem.*, 2011, **83**, 1232-1242.
10. R. Reisfeld, R. Zusman, Y. Cohen, and M. Eyal, *Chem. Phys. Lett.*, 1988, **147**, 142-147.

11. N. Banerji, S. Cowan, E. Vauthey, and A. J. Heeger, *J. Phys. Chem. C*, 2011, **115**, 9726-9739.
12. L. S. Forster and R. Livingston, *J. Chem. Phys.*, 1952, **20**, 1315-1320.
13. G. J. Hedley, A. J. Ward, A. Alekseev, C. T. Howells, E. R. Martins, L. A. Serrano, G. Cooke, A. Ruseckas, I. D. Samuel, *Nat Commun.*, 2013, **4**, 2867-2876.
14. W. Senevirathna and G. Sauvé, *J. Mater. Chem. C*, 2013, **1**, 6684-6694.